Calculated far-infrared lattice absorption spectra of cadmium telluride doped with beryllium

D. N. Talwar* and Bal K. Agrawal
Department of Physics, University of Allahabad, Allahabad 211002, India
(Received 4 September 1973)

The impurity-induced infrared lattice absorption has been calculated for a zinc-blende-type crystal in the low-concentration limit of substitutional impurities. The impurity is described by a nearest-neighbor perturbation model where along with the change in mass at the impurity site, the changes in the central and noncentral impurity-host crystal interactions have been considered. A numerical estimate has been made for impurity-induced infrared absorption in CdTe doped with Be impurities after employing a seven-parameter second-neighbor-ionic model. The main features of the experimentally observed absorption have been reasonably explained. The observed absorption peak at 61 cm^{-1} is seen to be an impurity-activated one-phonon acoustic band rather than a resonant mode suggested earlier by Sennett *et al.*

I. INTRODUCTION

In perfect alkali-halide crystals, the transverse-optical mode at the center of the Brillouin zone (BZ) (of essentially zero wave vector, i.e., $\vec{q}=0$) is infrared active predominantly when the light is incident perpendicular to the surface of the crystal.[1,2] One may also observe the longitudinal-optical mode of zero wave vector if the radiation is $\hat{p}$ polarized and incident obliquely to the crystal surface.[3] In the infrared-absorption spectrum, these fundamental bands (the well-known restrahlen absorption, in which a photon is supposed to be absorbed creating a lattice phonon) appear as sharp peaks. The translational symmetry is destroyed by the presence of impurities and the restrictive selection rule ($\vec{q}=0$) is relaxed. The incident radiation now interacts with nearly all the modes of the vibrational spectrum. There arise some additional absorption peaks in the phonon-band region due to the resonance modes[4] or outside the bands due to the localized or gap modes.[5]

In infrared studies of pure II-VI and III-V semiconductor compounds, in addition to the restrahlen absorption, several relatively weaker bands are also observed. Many authors[6–20] have seen such bands and have attributed them to processes involving more than one phonon for the case where the absorption peaks lie above the TO(Γ)-mode energy. If the weak bands lie below the TO(Γ)-mode energy, they are attributed to single- and multiple-phonon generation processes. The presence of impurities in these systems produces some additional absorption peaks which can easily be identified by making a comparison with the spectrum of the host system.

The infrared studies in pure CdTe have been made by several authors.[8–10,19] Recently, the absorption due to divalent Be impurities in CdTe has been measured by Sennett *et al.*,[21] who have detected an impurity-induced abosrption peak at 61 cm^{-1}. In order to understand the observed absorption these authors have performed a calculation in the mass-defect approximation and assumed that the impurity-induced absorption is proportional to the amplitude of the vibrating impurity. They predicted that the observed peak at 61 cm^{-1} is due to a resonance mode merely because a low density of states appears near this frequency.

The experimental data on the phonon dispersion of zinc-blende-type crystals is rather sparse even after the advent of neutron spectroscopy. Neutron data exist only for a few systems.[22–29] The dynamics of these compounds has been widely studied using both the phenomenological shell[22–25,27] and rigid-ion models.[30–37] The shell model, which had been seen to be very successful for discussing the lattice dyaamics of alkali halides, is not found to be the best one for the zinc-blende-type crystals. In particular, a shell model has been tried by Waugh and Dolling[22] for GaAs. In order to obtain good agreement with the experiment, it has been found necessary to incorporate a large number of disposable parameters. Some of these parameters have very little physical significance. The unique evaluation of the parameters can be made only if extreme restrictions are imposed on the model. It is evident from the fact that a somewhat simpler six-parameter shell model[24] fails to reproduce even approximate phonon dispersion relations in zinc sulphide crystals particularly for the optical modes. The applicability of the shell model for discussing the lattice dynamics of zinc-blende-type crystals has, in fact, been questioned by Dick[38] and Cochran[39] on basic grounds. These examples are intended to indicate the unsuitability of the shell model for a very reliable calculation of the phonon frequencies for crystals having ZnS crystal structure, particularly when insufficient experimental data are available.

The rigid-ion model (RIM), on the other hand, has general applicability to these solids and also has many computational advantages. A seven-parameter second-neighbor-ionic (SNI) model of Banerjee and Varshni[34] has earlier been seen to give a fair agreement with the neutron data in GaAs, GaP, CuCl,[34] ZnSe, InSb,[35] CuI,[37] and ZnS. It also works well in CdTe, ZnTe,[36] InP, InAs, and GaSb,[37] where very little experimental data are known. In earlier papers,[35-37] we have discussed the lattice dynamics of various II-VI and III-V semiconductor compounds and observed that the calculated phonon frequencies at the Bz boundaries agree well with the existing optical data. Furthermore, the SNI model is consistently superior to the simplified-force models.[40,41] The model has been found to be quite successful in explaining the thermodynamic properties[24,42] and the local-mode behavior due to various isoelectronic impurities in II-VI and III-V semiconductors.[43]

The purpose of the present paper is to calculate the absorption due to Be impurities in CdTe using a Green's-function method. The eigenvalues and eigenvectors of the phonons in CdTe have been calculated by employing the SNI lattice-dynamical model. It has been considered on chemical grounds that the Be ion occupies the Cd site in cadmium telluride crystals.[21,44] We assume a perturbation model where the mass of the impurity as well as the changes in the central-force constant between the impurity and its neighboring ions have been considered. As Be is a very light isoelectronic impurity in CdTe, a local mode has been observed at 391 cm^{-1}.[21,44] A mass-defect calculation performed earlier by the present authors[43] reproduced a value of 397 cm^{-1} for this local mode. This fact eventually reveals that the effects of force-constant changes in the CdTe: Be system may not be significant. A perusal of the phonon density of states indicates that the observed weak absorption peak at 61 cm^{-1} reflects the appropriate projection of the density of states of the host lattice (cf. Sec. IV C). A peak appears at 62 cm^{-1} in the one-phonon density of states because of the second highest acoustic band at the critical point K $[\frac{3}{4}, \frac{3}{4}, 0]$.

II. LATTICE DYNAMICS AND IMPURITY-INDUCED INFRARED LATTICE ABSORPTION

A. Lattice dynamics

Most of the $A^{II}B^{VI}$ compounds including CdTe exhibit the sphalerite (zinc-blende) crystal structure; the two kinds of atoms occupy the sites of two interpenetrating face-centered-cubic lattices. The two sublattices are oriented parallel to each other and displaced from one another by a vector $\frac{1}{2}a(1,1,1)$ where $2a$ is the edge length of the elementary cube of the face-centered lattice. The length of this vector is $\frac{1}{2}\sqrt{3}a \approx 0.866a$. The three basis vectors that define the rhombohedral parallelepiped unit cell are $\vec{a}_1 = a(1,1,0)$, $\vec{a}_2 = a(0,1,1)$, and $\vec{a}_3 = a(1,0,1)$. The volume of the unit cell is $2a^3$.

Figure 1 illustrates the zinc-blende crystal structure. The filled circles represent the atoms of the element of group II and are in lattice A. The open circles (the four nearest neighbors of a filled circle) represent the atoms of the element of group VI and are in lattice B.

The two atoms in the unit cell are labeled by the position vectors $\vec{R}_0 = \frac{1}{2}a(0,0,0)$ and $\vec{R}_1 = \frac{1}{2}a(1,1,1)$. Let the origin be a group-II atom. The four nearest-neighbor group-VI atoms are then given by

$$\vec{R}_1 = \tfrac{1}{2}a(1,1,1), \qquad \vec{R}_2 = \tfrac{1}{2}a(-1,-1,1),$$

$$\vec{R}_3 = \tfrac{1}{2}a(1,-1,-1), \quad \vec{R}_4 = \tfrac{1}{2}a(-1,1,-1).$$

The corresponding set for a group-VI atom lying at $\vec{R}_1$ would be

$$\vec{R}_0 = \tfrac{1}{2}a(0,0,0), \quad \vec{R}_5 = \vec{a}_1, \quad \vec{R}_6 = \vec{a}_2, \quad \vec{R}_7 = \vec{a}_3 .$$

The time-independent equations of motion for perfect ionic crystals in the harmonic approximation in matrix form are

$$(\overleftrightarrow{D}^{sc} - \omega^2 \overleftrightarrow{m}\,\overleftrightarrow{I})\vec{u} = 0 , \tag{1}$$

where ω is the phonon frequency, $\overleftrightarrow{m}$ is the diagonal matrix containing the masses of the constituent atoms m_κ ($\kappa = 1, 2$), $\overleftrightarrow{I}$ is the unit matrix, and $\overleftrightarrow{D}^{sc}$

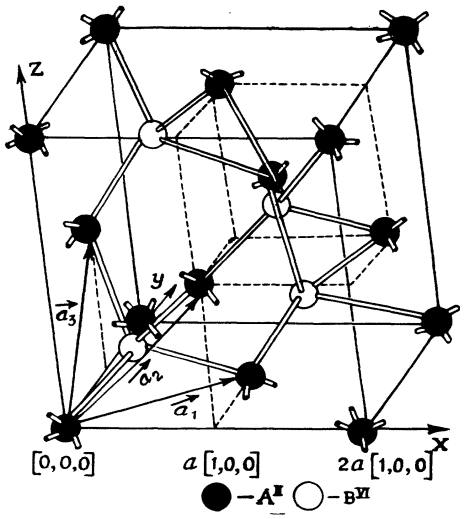

FIG. 1. Lattice structure of sphalerite (zinc-blende-type) crystals.

is the force-field matrix comprising the short-range interaction $\overleftrightarrow{D}^s$ and the Coulomb (long-range) interaction $\overleftrightarrow{D}^C$ matrices, respectively. The column vector $\vec{u}$ represents the atomic displacements.

Assuming the plane-wave solutions for the displacements of the κth atom of mass m_κ in the nth unit cell

$$u(n\kappa) = \frac{1}{(Nm_\kappa)^{1/2}}\, e_\alpha(\kappa|\vec{q}, s)\, e^{i\vec{q}\cdot\vec{R}(n\kappa)}\ , \tag{2}$$

Eq. (1) becomes

$$(\overleftrightarrow{C} - \omega^2 \overleftrightarrow{I})\vec{e} = 0\ . \tag{3}$$

Here the polarization vector $\vec{e}$ has the Cartesian components $e_\alpha(\kappa|\vec{q}, s)$ at site κ for the wave vector $\vec{q}$ in the polarization branch s. N is the number of unit cells in the crystal; $\vec{R}(n\kappa)$ is the position vector of the lattice site $(n\kappa)$; $\overleftrightarrow{C}$ is the Fourier-transformed dynamical matrix whose elements are

$$C_{\alpha\beta}(\vec{q}|\,\kappa\kappa') = \sum_{\bar{n}} L^0_{\alpha\beta}(\bar{n}|\,\kappa\kappa')\, e^{-i[\vec{q}\cdot\vec{R}(\bar{n})]}\ , \tag{4}$$

where $\bar{n} = (n\kappa) - (n'\kappa')$ and $\vec{R}(\bar{n}) = \vec{R}(n\kappa) - \vec{R}(n'\kappa')$ denotes the differences of the position vectors of the two lattice sites $(n\kappa)$ and $(n'\kappa')$. The elements of the mass-reduced dynamical matrix are given by

$$L^0_{\alpha\beta}(\bar{n}|\,\kappa\kappa') = D^{s\,C}_{\alpha\beta}(n\kappa; n'\kappa')/(m_\kappa m_{\kappa'})^{1/2}\ . \tag{5}$$

The solutions of Eq. (3) are the frequencies ω as a function of the wave vector $\vec{q}$, i.e., the dispersion curves of the host lattice. For each $\omega(\vec{q}, s)$ the polarization vectors satisfy the familiar orthogonality and closure relations

$$\begin{aligned} &\sum_\alpha e^*_\alpha(\kappa|\vec{q}, s) e_\alpha(\kappa|\vec{q}, s') = \delta_{ss'}\ , \\ &\sum_s e^*_\alpha(\kappa|\vec{q}, s) e_\beta(\kappa|\vec{q}, s) = \delta_{\alpha\beta}\ . \end{aligned} \tag{6}$$

Now returning to Eq. (1) we may write it as

$$\overleftrightarrow{L}^0\vec{\psi} = \omega^2 \overleftrightarrow{I}\,\vec{\psi}\ , \tag{7}$$

where

$$\overleftrightarrow{L}^0 = (\overleftrightarrow{m})^{-1/2}\overleftrightarrow{D}^{s\,C}(\overleftrightarrow{m})^{-1/2}$$

and $\vec{\psi}$ is a column vector related to the atomic displacement vector $\vec{u}$ by

$$\vec{u} = (\overleftrightarrow{m})^{-1/2}\vec{\psi}\ . \tag{8}$$

For a crystal containing defects the equation of motion may be written

$$[\overleftrightarrow{L}^0 + \overleftrightarrow{P}(\omega^2)]\vec{\psi}' = \omega^2 \overleftrightarrow{I}\,\vec{\psi}'\ , \tag{9}$$

where $\overleftrightarrow{P}(\omega^2)$ is the perturbation matrix due to the defects. Its explicit form is

$$\begin{aligned} \overleftrightarrow{P}(\omega^2) = &-\omega^2(\overleftrightarrow{m})^{-1/2}\Delta\overleftrightarrow{m}(\overleftrightarrow{m})^{-1/2} \\ &+ (\overleftrightarrow{m})^{-1/2}\Delta\overleftrightarrow{D}^s(\overleftrightarrow{m})^{-1/2}\ . \end{aligned} \tag{10}$$

Here the mass and the force-constant matrices of the imperfect crystal have been written as $(\overleftrightarrow{m} + \Delta\overleftrightarrow{m})$ and $(\overleftrightarrow{D}^{s\,C} + \Delta\overleftrightarrow{D}^s)$, respectively, and $\vec{\psi}'$ is the displacement vector of the imperfect lattice.

B. Impurity-induced infrared lattice absorption

The impurity induced ir absorption in crystals has been discussed by several authors.[1,2,46,47] For a harmonic crystal the extra absorption due to a single impurity is given by

$$\begin{aligned} \alpha(\omega) = &\frac{4\pi\{n^2(\infty)+2\}^2\omega}{9n(\omega)}\ \frac{N}{Vc}\ \frac{e^{*2}_{\text{eff}}}{\hat{\mu}} \\ &\times \mathrm{Im}\langle 0, \mathrm{TO}|\,\overleftrightarrow{G}(z)|\,0, \mathrm{TO}\rangle\ , \end{aligned} \tag{11}$$

where $n^2(\infty)$ is the high-frequency dielectric constant, $n^2(\omega)$ is the dielectric constant at the frequency ω, c is the velocity of light, N is the number of unit cells in the crystal volume V, e^*_{eff} is the effective charge (taken as Szigetti's effective charge[48] equal to 0.72 for the pure CdTe crystal), $\hat{\mu}$ is the reduced mass of an unit cell, $\overleftrightarrow{G}(z)\{\equiv[\overleftrightarrow{L}^0 + \overleftrightarrow{P}(\omega^2) - z\overleftrightarrow{I}]^{-1}\}$ is the Green's-function matrix for the crystal containing the impurities, and $|0, \mathrm{TO}\rangle$ is a normalized eigenvector of the $\vec{q} = 0$ TO phonon in one direction.

The Green's-function matrix for the imperfect crystal is related to the Green's-function matrix for the perfect crystal by the Dyson equation

$$\begin{aligned} \overleftrightarrow{G}(z) &= \overleftrightarrow{G}^0(z)[\overleftrightarrow{I} + \overleftrightarrow{G}^0(z)\overleftrightarrow{P}(\omega^2)]^{-1}\ , \\ &= \overleftrightarrow{G}^0(z) - \overleftrightarrow{G}^0(z)\overleftrightarrow{P}(\omega^2)\overleftrightarrow{G}^0(z) \\ &\quad + \overleftrightarrow{G}^0(z)\overleftrightarrow{P}(\omega^2)\overleftrightarrow{G}^0(z)\overleftrightarrow{P}(\omega^2)\overleftrightarrow{G}^0(z) - \cdots\ , \\ &\equiv \overleftrightarrow{G}^0(z) - \overleftrightarrow{G}^0(z)\overleftrightarrow{T}(z)\overleftrightarrow{G}^0(z)\ , \end{aligned} \tag{12}$$

where the T matrix is defined by

$$\overleftrightarrow{T}(z) = \overleftrightarrow{P}(\omega^2)[\overleftrightarrow{I} + \overleftrightarrow{G}^0(z)\overleftrightarrow{P}(\omega^2)]^{-1}\ . \tag{13}$$

The resonance denominator contained in the inverse matrix $[\overleftrightarrow{I} + \overleftrightarrow{G}^0(\omega)\overleftrightarrow{P}(\omega^2)]^{-1}$ is of central importance for the investigation of the impurity modes. By separating its real and imaginary parts we have

$$\begin{aligned} D(z) &= \det|\,\overleftrightarrow{I} + \overleftrightarrow{G}^0(z)\overleftrightarrow{P}(\omega^2)| \\ &= \mathrm{Re}D(z) + i\,\mathrm{Im}D(z)\ . \end{aligned} \tag{14}$$

The frequencies of the localized, gap, or resonance modes are the solutions of the equation

$$\mathrm{Re}D(z) = 0\ . \tag{15}$$

Using Eqs. (11)–(13) along with the relation

$\vec{G}^0(z)|0, TO\rangle = (\omega_0^2 - z)^{-1}|0, TO\rangle$, the impurity induced ir absorption due to a randum distribution of a fractional concentration $[p]$ of impurity ions is seen to be

$$\alpha(\omega) = -\frac{4\pi\{n^2(\infty)+2\}^2}{9n(\omega)} \frac{\omega}{(\omega_0^2-\omega^2)^2} \frac{pe_{\text{eff}}^{*2}}{c\hat{\mu}\Omega} \operatorname{Im} t_{00}(z) , \tag{16}$$

where Ω denotes the volume of the unit cell. The scalar product $t_{00}(z)$ is the matrix element of the T matrix (in F_2 irreducible representation; see Sec. III) for the $\vec{q}=0$ transverse-optic mode and is given by

$$t_{00}(z) = \hat{\mu}\left[\frac{t_{11}}{m(\pm)} + \frac{4t_{22}}{m(\mp)} + \frac{8t_{33}}{m(\mp)} + \frac{8\sqrt{2}t_{23}}{m(\mp)} - \frac{4\sqrt{2}t_{13}}{[m(\pm)m(\mp)]^{1/2}} - \frac{4t_{12}}{[m(\pm)m(\mp)]^{1/2}}\right] \tag{17}$$

for a zinc-blende-type crystal. The (+) or (−) sign in $m(\pm)$ denotes the mass of the positively or the negetively charged ion. The upper or lower signs in Eq. (17) are to be taken for an impurity lying at a (+) or (−) ion site.

III. DEFECT PERTURBATION MODEL

For the case of a single impurity in the lattice, the nonzero elements of the perturbation matrix lie only in the space occupied by the impurity and its immediate neighbors, i.e., the "impurity space." If b is the number of atoms directly perturbed by the impurity including the impurity ion itself, the perturbation matrix $\vec{P}(\omega^2)\{\equiv \vec{p}(\omega^2)\}$ is of dimension $3b\times 3b$. In the present case we assume that the impurity occupies the site of a group-II atom and consider the changes in the nearest-neighbor central and noncentral interactions. The matrix elements of the perturbation matrix of dimension 15×15 are

$$\begin{aligned}
&p_{ii}(\vec{0},\vec{0}) = -\epsilon\omega^2 + \tfrac{4}{3}(\lambda+2\lambda'),\\
&p_{ij}(\vec{0},\vec{0}) = 0,\\
&p_{ii}(\vec{0},\vec{R}_n) = -\tfrac{1}{3}\chi^{1/2}(\lambda+2\lambda'),\\
&p_{ij}(\vec{0},\vec{R}_n) = -\tfrac{1}{3}\chi^{1/2}(\lambda-\lambda')n_i n_j ,\\
&p_{ii}(\vec{R}_n,\vec{R}_n) = \tfrac{1}{3}\chi(\lambda+2\lambda'),\\
&p_{ij}(\vec{R}_n,\vec{R}_n) = \tfrac{1}{3}\chi(\lambda-\lambda')n_i n_j ,
\end{aligned} \tag{18}$$

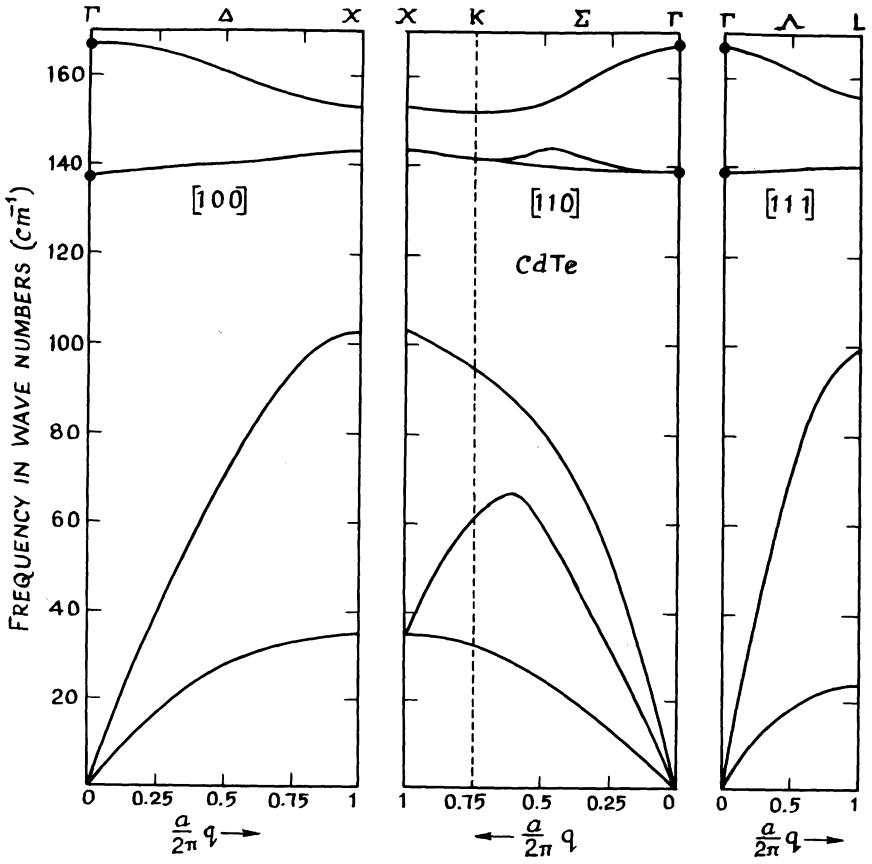

FIG. 2. Calculated dispersion curves of CdTe. Solid dots (●) denote the infrared data, Ref. 52. The points Γ, X, L, W, K, Σ, Δ, and Λ denote the critical points in the Brillouin zone.

$i,j = 1, 2, 3$, where $\epsilon = [m'(\pm) - m(\pm)]/m(\pm)$ is the mass-change parameter, $\chi = m(\pm)/m(\mp)$ is the ratio of the masses of the ions of the two sublattices, $\lambda = \Delta\alpha/m(\pm)$ and $\lambda' = \Delta\beta/m(\pm)$ are the changes in the mass-reduced central and noncentral nearest-neighbor force constants (α and β are the nearest-neighbor central and noncentral force constants of the deLauney type in the host lattice) in units of squared frequency, and $\vec{R}_n[=\frac{1}{2}a \times (n_1, n_2, n_3)]$ is the lattice vector of the nearest neighbor of the impurity site.

The irreducible representations which appear for an impurity site having $[T_d]$ symmetry in the zinc-blende-type lattice are F_2, F_1, A_1, and E. The necessary symmetry coordinates, i.e., the symmetrized linear combinations of the 15 ionic displacements in the impurity space have been worked out by Ludwig.[49] The normal modes which are infrared active are those which transform according to the F_2 irreducible representation. The matrix elements of $\overleftrightarrow{p}(\omega^2)$ in the F_2 representation are

$$\overleftrightarrow{p}_{F_2}(\omega^2) = \begin{pmatrix} -\epsilon\omega^2 + \frac{4}{3}(\lambda + 2\lambda') & -\frac{2}{3}\chi^{1/2}(\lambda + 2\lambda') & -\frac{2}{3}\sqrt{2}\,\chi^{1/2}(\lambda - \lambda') \\ -\frac{2}{3}\chi^{1/2}(\lambda + 2\lambda') & \frac{1}{3}\chi(\lambda + 2\lambda') & \frac{1}{3}\sqrt{2}\,\chi(\lambda - \lambda') \\ -\frac{2}{3}\sqrt{2}\,\chi^{1/2}(\lambda - \lambda') & \frac{1}{3}\sqrt{2}\,\chi(\lambda - \lambda') & \frac{1}{3}\chi(2\lambda + \lambda') \end{pmatrix} . \tag{19}$$

We define a Green's-function matrix for the unperturbed crystal by $\overleftrightarrow{G}^0(z)\{\equiv[\overleftrightarrow{L}^0 - z\overleftrightarrow{I}]^{-1}\}$, where z is the complex frequency, $z = \omega^2 + 2i\zeta$ in the limit as $\zeta \to 0^+$. The matrix elements of the Green's function matrix $\overleftrightarrow{g}(z)$ in the F_2 irreducible representation are seen to be

$$\overleftrightarrow{g}_{F_2}(z) = \begin{pmatrix} g_1(\pm) & 2g_3(\pm) & 2\sqrt{2}\,g_4(\pm) \\ 2g_3(\pm) & [g_2(\pm) + 2g_5(\pm) + g_6(\pm)] & \sqrt{2}\,g_7(\pm) \\ 2\sqrt{2}\,g_4(\pm) & \sqrt{2}\,g_7(\pm) & [g_2(\pm) - g_6(\pm) - g_7(\pm) - 2g_8(\pm)] \end{pmatrix} , \tag{20}$$

where

$$\begin{aligned} g_1(\pm) &= g_{xx}(0,0,0;0,0,0), \\ g_2(\pm) &= g_{xx}(1,1,1;1,1,1), \\ g_3(\pm) &= g_{xx}(0,0,0;1,1,1), \\ g_4(\pm) &= g_{xy}(0,0,0;1,1,1), \\ g_5(\pm) &= g_{xx}(1,1,1;-1,-1,1), \\ g_6(\pm) &= g_{zz}(1,1,1;-1,-1,1), \\ g_7(\pm) &= g_{xy}(1,1,1;-1,-1,1), \\ g_8(\pm) &= g_{xz}(1,1,1;-1,-1,1) . \end{aligned} \tag{21}$$

The different elements of Green's function matrix $g(\pm;z)$ are given by

$$g_\xi(\pm;z) = \frac{1}{N}\sum_{\vec{q}}\sum_{s}\frac{j_\xi(\pm|\vec{q},s)}{\omega^2(\vec{q},s) - z} , \tag{22a}$$

where $\xi = 1$ to 8 and the complex quantities $j_\xi(\pm|\vec{q},s)$ stand for the following expression:

$$j_1(\pm|\vec{q},s) = \begin{cases} \mathrm{Re}j_1(\pm|\vec{q},s) = [\mathrm{Re}e_\alpha(\pm|\vec{q},s)]^2 + [\mathrm{Im}e_\alpha(\pm|\vec{q},s)]^2 \\ \mathrm{Im}j_1(\pm|\vec{q},s) = 0, \end{cases}$$

$$j_2(\pm|\vec{q},s) = \begin{cases} \mathrm{Re}j_2(\pm|\vec{q},s) = \mathrm{Re}j_1(\mp|\vec{q},s) \\ \mathrm{Im}j_2(\pm|\vec{q},s) = 0, \end{cases}$$

$$j_3(\pm|\vec{q},s) = \begin{cases} \mathrm{Re}j_3(\pm|\vec{q},s) = [A_1\cos\tfrac{1}{2}q_\alpha a\cos\tfrac{1}{2}q_\beta a\cos\tfrac{1}{2}q_\gamma a - B_1\sin\tfrac{1}{2}q_\alpha a\sin\tfrac{1}{2}q_\beta a\sin\tfrac{1}{2}q_\gamma a] \\ \mathrm{Im}j_3(\pm|\vec{q},s) = [A_1\sin\tfrac{1}{2}q_\alpha a\sin\tfrac{1}{2}q_\beta a\sin\tfrac{1}{2}q_\gamma a + \bar{B}_1\cos\tfrac{1}{2}q_\alpha a\cos\tfrac{1}{2}q_\beta a\cos\tfrac{1}{2}q_\gamma a], \end{cases}$$

$$j_4(\pm|\vec{q},s) = \begin{cases} \mathrm{Re}j_4(\pm|\vec{q},s) = -[A_2\sin\tfrac{1}{2}q_\alpha a\sin\tfrac{1}{2}q_\beta a\cos\tfrac{1}{2}q_\gamma a - B_2\cos\tfrac{1}{2}q_\alpha a\cos\tfrac{1}{2}q_\beta a\sin\tfrac{1}{2}q_\gamma a] \\ \mathrm{Im}j(\pm|\vec{q},s) = -[A_2\cos\tfrac{1}{2}q_\alpha a\cos\tfrac{1}{2}q_\beta a\sin\tfrac{1}{2}q_\gamma a + B_2\sin\tfrac{1}{2}q_\alpha a\sin\tfrac{1}{2}q_\beta a\cos\tfrac{1}{2}q_\gamma a] , \end{cases}$$

$$j_5(\pm|\vec{q},s)=\begin{cases}\mathrm{Re}j_5(\pm|\vec{q},s)=\mathrm{Re}j_2(\pm|\vec{q},s)\cos\frac{1}{2}(2q_\alpha+q_\beta+q_\gamma)a\cos\frac{1}{2}(q_\beta-q_\gamma)a\\ \mathrm{Im}j_5(\pm|\vec{q},s)=\mathrm{Re}j_2(\pm|\vec{q},s)\sin\frac{1}{2}(2q_\alpha+q_\beta+q_\gamma)a\cos\frac{1}{2}(q_\beta-q_\gamma)a\,,\end{cases}$$

$$j_6(\pm|\vec{q},s)=\begin{cases}\mathrm{Re}j_6(\pm|\vec{q},s)=\mathrm{Re}j_2(\pm|\vec{q},s)\cos(q_\beta+q_\gamma)a\\ \mathrm{Im}j_6(\pm|\vec{q},s)=\mathrm{Re}j_2(\pm|\vec{q},s)\sin(q_\beta+q_\gamma)a,\end{cases}$$

$$j_7(\pm|\vec{q},s)=\begin{cases}\mathrm{Re}j_7(\pm|\vec{q},s)=[A_3\cos(q_\alpha+q_\beta)a-B_3\sin(q_\alpha+q_\beta)a]\\ \mathrm{Im}j_7(\pm|\vec{q},s)=[A_3\sin(q_\alpha+q_\beta)a+B_3\cos(q_\alpha+q_\beta)a]\,,\end{cases}$$

$$j_8(\pm|\vec{q},s)=\begin{cases}\mathrm{Re}j_8(\pm|\vec{q},s)=-[A_3\sin\frac{1}{2}(q_\alpha+q_\beta+2q_\gamma)a+B_3\cos\frac{1}{2}(q_\alpha+q_\beta+2q_\gamma)a]\sin\frac{1}{2}(q_\alpha-q_\beta)a\\ \mathrm{Im}j_8(\pm|\vec{q},s)=[A_3\cos\frac{1}{2}(q_\alpha+q_\beta+2q_\gamma)a-B_3\sin\frac{1}{2}(q_\alpha+q_\beta+2q_\gamma)a]\sin\frac{1}{2}(q_\alpha-q_\beta)a\,,\end{cases}\tag{22b}$$

where $\alpha,\ \beta,\ \gamma=1,\ 2,\ 3$ but $\alpha\neq\beta\neq\gamma$, and $e_\alpha(\pm|\vec{q},s)\equiv\mathrm{Re}e_\alpha(\pm|\vec{q},s)+i\,\mathrm{Im}e_\alpha(\pm|\vec{q},s)$. Further,

$$A_1=\mathrm{Re}e_\alpha(\pm|\vec{q},s)\,\mathrm{Re}e_\alpha(\mp|\vec{q},s)+\mathrm{Im}e_\alpha(\pm|\vec{q},s)\,\mathrm{Im}e_\alpha(\mp|\vec{q},s),$$

$$B_1=\mathrm{Re}e_\alpha(\mp|\vec{q},s)\,\mathrm{Im}e_\alpha(\pm|\vec{q},s)-\mathrm{Re}e_\beta(\pm|\vec{q},s)\,\mathrm{Im}e_\alpha(\mp|\vec{q},s),$$

$$A_2=\mathrm{Re}e_\alpha(\pm|\vec{q},s)\,\mathrm{Re}e_\beta(\mp|\vec{q},s)+\mathrm{Im}e_\alpha(\pm|\vec{q},s)\,\mathrm{Im}e_\beta(\mp|\vec{q},s),$$

$$B_2=\mathrm{Re}e_\beta(\mp|\vec{q},s)\,\mathrm{Im}e_\alpha(\pm|\vec{q},s)-\mathrm{Re}e_\alpha(\pm|\vec{q},s)\,\mathrm{Im}e_\beta(\mp|\vec{q},s),$$

$$A_3=\mathrm{Re}e_\alpha(\mp|\vec{q},s)\,\mathrm{Im}e_\beta(\mp|\vec{q},s)+\mathrm{Im}e_\alpha(\mp|\vec{q},s)\,\mathrm{Im}e_\beta(\mp|\vec{q},s),$$

$$B_3=\mathrm{Im}e_\alpha(\mp|\vec{q},s)\,\mathrm{Re}e_\beta(\mp|\vec{q},s)-\mathrm{Re}e_\alpha(\mp|\vec{q},s)\,\mathrm{Im}e_\beta(\mp|\vec{q},s)\,.$$

IV. NUMERICAL COMPUTATIONS

A. Phonons

We have employed a SNI–lattice-dynamical model for the computation of the eigenfrequencies and the eigenvectors of the host CdTe crystal. The model incorporates the short-range forces[40] (up to and including the second neighbors) and the long-range Coulomb forces.[50] The elements of the short-range interaction matrix depend on the model parameters α, β, μ_1, μ_2, λ_1, λ_2, and the masses of the constituent atoms and the lattice constant. The elements of the long-range Coulomb interaction matrix are related to the effective charge and the lattice parameters of the crystal. For details we refer to an earlier paper.[36]

The evaluation of the involved seven lattice-dynamical model parameters is usually made by using the data of phonon frequencies at critical-points (Γ and X) as an input with the three experimentally determined elastic constants as constraints on the values of the parameters. The expressions relating the three elastic constants with the model parameters are

$$2ac_{11}=0.1255\chi+\alpha+4(\mu_1+\mu_2),\tag{23}$$

$$2ac_{12}=1.324\chi+2\beta-\alpha-2(\lambda_1+\lambda_2)+2(\mu_1+\mu_2),\tag{24}$$

and

$$2ac_{44}=-0.063\chi+\alpha+2(\lambda_1+\lambda_2)+2(\mu_1+\mu_2)-2aA^2/B\,,\tag{25}$$

with

$$2a\frac{A^2}{B}\equiv\frac{(1.2595\chi-\beta)^2}{\alpha-\pi\chi/6}\,.$$

As mentioned earlier, no detailed neutron scattering data are available for CdTe, and consequently one does not know the exact critical-phonon frequencies required for the evaluation of the seven parameters in this model. We have, thus, adopted alternative approaches to seek a guideline for the critical-point phonon frequencies.

A very good source of the TO(Γ)-mode frequencies for the long-wavelength vibrations is the study of the infrared reflection or absorption spectrum.[6–21] The zone center LO(Γ)-mode frequency $\omega_{\mathrm{LO}(\Gamma)}$ may be evaluated by using the well-known Lyddane–Sachs–Teller (LST) relationship,[51] $\omega_{\mathrm{LO}(\Gamma)}=\{n^2(\omega)/n^2(\infty)\}^{1/2}\omega_{\mathrm{TO}(\Gamma)}$. In zinc-blende-type crystals, the long-wavelength optical vibrational modes are allowed (by the selection rules[2]) to be Raman active, and, therefore, the first- or second-order Raman scattering measurements are most suitable to obtain the optical-mode frequencies at the center of the Brillouin zone. Quite recently, Beserman and Balkanski[52] have observed

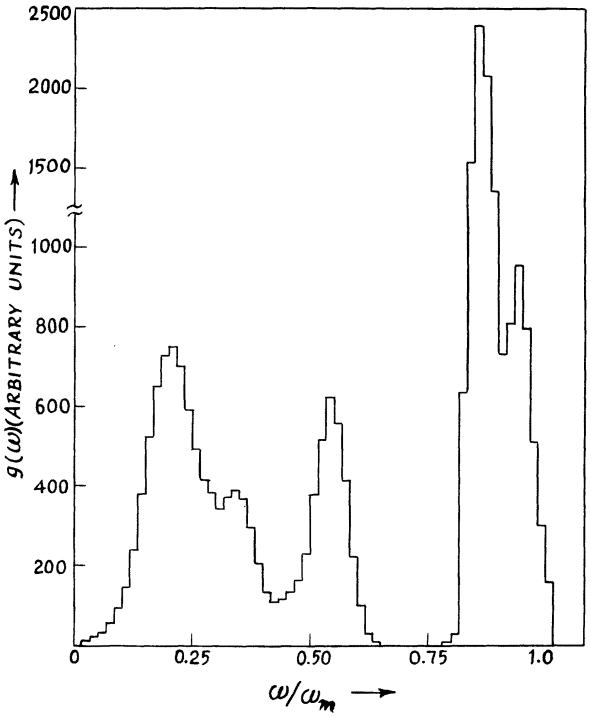

FIG. 3. Calculated one-phonon density of states of CdTe.

the zone-center phonon frequencies in the infrared reflection spectrum of ZnSe, ZnTe, and CdTe crystals. These frequencies are in close agreement with those measured by first- or second-order Raman scattering experiments.[19,53-56]

In order to obtain the critical-point phonons from the optical measurements (infrared or second-order Raman spectrum) it is essential to perform a correct analysis. In the absence of the neutral data or reliable lattice-dynamical calculations, wrong assignments of the observed peaks in terms of the critical-point phonons have been made in the past.[8-10] In the absence of the neutron data it is worthwile to calculate the zone-boundary phonon energies from the reliable theoretical approaches. We have followed the following approaches to get the optical and acoustical zone-boundary phonon energies:

1. Optical- and acoustical-phonon energies

An approximate estimation of the longitudinal-optical or -acoustical phonon energies at critical point X can be made by plotting values of these phonons already known either from the neutron scattering or Raman scattering experiments as a function of $(2ac_{11}/m_1)^{1/2}$ or $(2ac_{11}/m_2)^{1/2}$ for various compounds having zinc-blende-type crystal structures $m_1 < m_2$ (see Figs. 1 and 2 of Ref. 36). Both of these curves are seen to be approximately linear. The calculated values of $(2ac_{11}/m_1)^{1/2}$ and $(2ac_{11}/m_2)^{1/2}$ for the system under study, in turn, give the LO(X) and LA(X) phonon energies. Our calculated values, when compared with the existing second-order Raman and other optical measurements, are found to be reasonably good. For details we refer to an earlier paper.[36]

2. Acoustical-phonon energies

The dispersion relations for II-VI [ZnS and ZnSe] and III-V semiconductor compounds [GaS, GaP, InSb, InP (for acoustical branches only)]

TABLE I. Acoustic- and optical-phonon energies at various critical points as calculated by the SNI–lattice-dynamical model. The available optical data and the calculated results of Sennett *et al.* (Ref. 21) are also presented for comparison. All the phonon energies are in wave numbers (cm^{-1}).

Critical points	Lattice mode	Lattice-dynamical calculations: SNI model	Lattice-dynamical calculations: Shell model[a] (Ref. 21)	Optical data
Γ	LO	167	171	167[b]
	TO	139	140	139[b]
X	LO	153	137	•••
	TO	143	163	•••
	LA	103	125	•••
	TA	35	50	36[c]
L	LO	156	147	•••
	TO	140	155	•••
	LA	100	110	104.5[c]
	TA	24	35	25[c]
W	W_1	51	52	•••
	W_2	57	56	•••
	W_3	91	118	•••
	W_4	139	135	•••
	W_5	144	165	•••
	W_6	152	165	•••
Σ	Σ_1	20	•••	•••
	Σ_2	46	•••	46[c]
	Σ_3	70	•••	•••
	Σ_4	139	•••	•••
	Σ_5	142	•••	•••
	Σ_6	158	•••	•••
K	K_1	32	42	•••
	K_2	62	60	•••
	K_3	94	116	•••
	K_4	141	137	•••
	K_5	142	160	•••
	K_6	153	165	•••

[a]Approximate values of phonon energies have been read from the calculated dispersion curves by Sennett *et al.* (Ref. 21).

[b]Reference 52 and M. Balkanski, R. Beserman, and L. K. Vodopianov, in *Localized Excitations in Solids*, edited by R. F. Wallis (Plenum, New York, 1968), p. 154.

[c]G. A. Slack and S. Roberts, Phys. Rev. B 3, 2613 (1971).

have been carefully studied by neutron scattering techniques. By plotting the dispersion of acoustical phonons along the (1, 0, 0) direction for any one of these compounds, the slopes of the dispersion curves near $\vec{q}=0$ can be extrapolated to give the linear-limit values. However, these linear-limit energies can also be calculated from the experimentally determined elastic constants by the relations[57]

$$\lim_{q\to 0}(\omega_{LA(X)})=\left(\frac{c_{11}}{\rho}\right)^{1/2}\frac{1}{2ac} \tag{26}$$

and

$$\lim_{q\to 0}(\omega_{TA(X)})=\left(\frac{c_{44}}{\rho}\right)^{1/2}\frac{1}{2ac}\ , \tag{27}$$

where ρ is the crystal density and $\lim_{q\to 0}(\omega_{LA(X)})$ and $\lim_{q\to 0}(\omega_{TA(X)})$ are the linear-limit longitudinal and transverse-acoustical phonon energies at critical point X.

The acoustical-phonon energies can be correlated to the above linear limiting values as

$$\omega_{LA(X)}=C_1\lim_{q\to 0}(\omega_{LA(X)}) \tag{28}$$

and

$$\omega_{TA(X)}=C_2\lim_{q\to 0}(\omega_{TA(X)})\ , \tag{29}$$

where C_1 and C_2 are the unknown constants having positive values less than unity. These constants have been evaluated from the known dispersion curves for the acoustical-phonon branches in other compounds and are taken to be same for the system under study. It is found that the LA(X) phonon energy calculated in this manner and by the procedure described above is very much similar

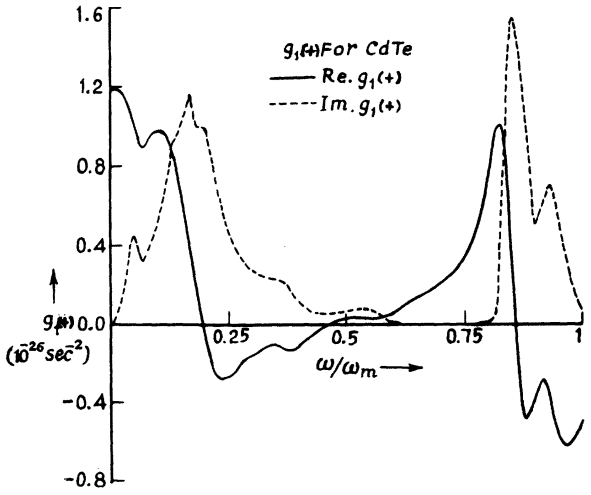

FIG. 4. Calculated real and imaginary parts of the Green's function $g_1(+)$ for CdTe.

to the existing optical data. The same is true for the case of the TA(X) phonon energy. For details we refer to earlier papers.[36,37]

With the help of the Brout sum rule,[58] the value of the TO(X) energy can be calculated after using the optical data for the energies at the center of the BZ and the calculated values of the energies of LO(X), LA(X), and TA(X) phonons.

In the calculation of the involved parameters for the lattice-dynamical–SNI model we have deviated a bit from the usual procedure of Banerjee and Varshni.[34] Two of the model parameters α and χ are calculated using the LO(Γ) and TO(Γ) phonon frequencies by the relations

$$\alpha=\tfrac{1}{12}\hat{\mu}[\omega^2_{LO(\Gamma)}+2\omega^2_{TO(\Gamma)}] \tag{30a}$$

and

$$\chi=(\hat{\mu}/2\pi)[\omega^2_{LO(\Gamma)}-\omega^2_{TO(\Gamma)}]\ . \tag{30b}$$

The parameter μ_1 is calculated using the LO(X) phonon frequency from the relation

$$\mu_1=\tfrac{1}{4}[\tfrac{1}{4}m_1\omega^2_{LO(X)}-\alpha-0.54125\chi]\ . \tag{31}$$

Now the parameter μ_2 is calculated using Eq. (23) in such a way that it reproduces a reasonable value of LA(X). Approximate values of β and $(\lambda_1+\lambda_2)$ are then calculated from the remaining two equations of elastic constants, (24) and (25). The values of the parameters and the transverse-optical and -acoustical phonon energies at critical point X are adjusted to have an independent calculation of the parameters λ_1 and λ_2 from the relations

$$\lambda_1=\frac{m_1}{8}\left\{\left(\frac{\omega^2_{TO(X)}+\omega^2_{TA(X)}}{2}\right)+\left[\left(\frac{\omega^2_{TO(X)}-\omega^2_{TA(X)}}{2}\right)^2-\frac{(4\beta-5.335\chi)^2}{m_1m_2}\right]^{1/2}-\frac{4}{m_1}(\alpha+2\mu_1-0.27\chi)\right\}\ , \tag{32}$$

and

$$\lambda_2=\frac{m_2}{8}\left\{\left(\frac{\omega^2_{TO(X)}+\omega^2_{TA(X)}}{2}\right)-\left[\left(\frac{\omega^2_{TO(X)}-\omega^2_{TA(X)}}{2}\right)^2-\frac{(4\beta-5.335\chi)^2}{m_1m_2}\right]^{1/2}-\frac{4}{m_2}(\alpha+2\mu_2-0.27\chi)\right\}\ . \tag{33}$$

During the evaluation it is kept in mind that the values of λ_1 and λ_2 should reproduce reasonable values of the zone-boundary phonon energies. The macroscopic data used in the calculation of the unknown parameters along with the calculated parameters for CdTe have been given in an earlier paper.[36]

The translational vector of the reciprocal space was divided into 16 equal parts to give rise to a

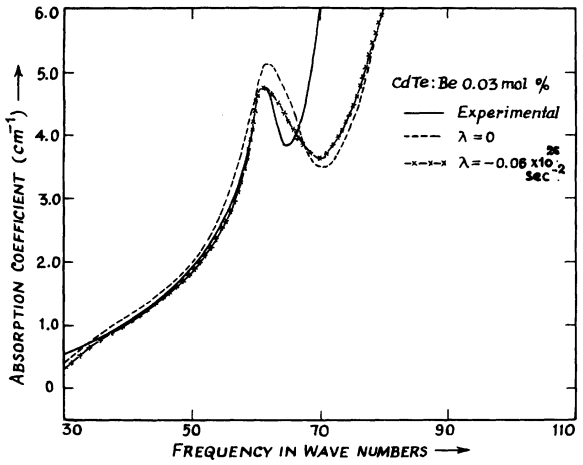

FIG. 5. Calculated impurity-induced infrared absorption.

grid of 4096 equally spaced points inside the first BZ. Because of the symmetry considerations of the BZ for the zinc-blende structure it is only necessary to determine the frequencies in the range

$$\vec{q} = (\pi/2a)\tfrac{1}{16}(q_x, q_y, q_z), \tag{34}$$

where q_x, q_y, and q_z are positive integers and satisfy the following inequalities:

$$0 \leq q_x \leq q_y \leq q_z \leq 16\ ,$$

and

$$|q_x + q_y + q_z| \leq 24. \tag{35}$$

There are 149 points defined by these numbers in the $\frac{1}{48}$th part of the BZ.

The calculated phonon dispersion curves along the three symmetry, [100], [110], and [111], directions and the resulting one-phonon density of states have been displayed in Figs. 2 and 3, respectively. The calculated zone-boundary phonon frequencies along with the existing optical data are given in Table I.

B. Green's functions

In the calculation of the complex-valued Green's functions, a staggered-bin averaging procedure has been followed. First, the quantities given in Eq. (22b) were calculated and sorted out by dividing the frequency interval into 60 equal bins. The resulting histograms are used to calculate the real and imaginary parts of the Green's functions at low frequencies. To carry out the actual integration of the real part of the Green's functions at low frequencies, the method of Sievers *et al.*[59] has been followed.

In the integrations the frequency increment is chosen in such a way that the spurious fluctuations appearing in the Green's functions are minimized. For the present choice of 4096 points in the first BZ, a value of 0.35 for the frequency increment in units of bin was seen to be appropriate. As a representative case the real and imaginary parts of the Green's function $g_1(+)$ have been shown in Fig. 4.

C. Absorption coefficient

Using Eq. (16) we have performed numerical calculations for the impurity-induced infrared absorption in CdTe crystal doped with 0.03-mol% Be impurities. The experimental and the calculated absorption curves are shown in Fig. 5. It is noted that the position and the general shape of the peak in the experimental spectra has been achieved even in the mass-defect approximation, but the calculated absorption exhibits a relatively lower height than the observed one. The calculated absorption curve has thus been scaled by a factor of 1.7 so as to facilitate comparison with the observed absorption. In order to obtain a better fit and a sharper peak we have calculated the absorption by considering changes in the central-force constant. The most appropriate value for the central-force-constant change is found to be $\lambda = -0.06\times10^{26}$ sec^{-2}. It corresponds to a ~5.5% reduction in the nearest-neighbor central force constant [$\alpha/m(+) = 1.108\times10^{26}$ sec^{-2}]. It reproduces the position and the height of the peak at 62 cm^{-1} fairly well. The real part of the resonance denominator $\mathrm{Re}D_{F_2}(z)$ has been plotted in Fig. 6 after considering the mass change as well as the force-constant change. No resonance mode appears in the low-frequency region, e.g., at 61 cm^{-1},

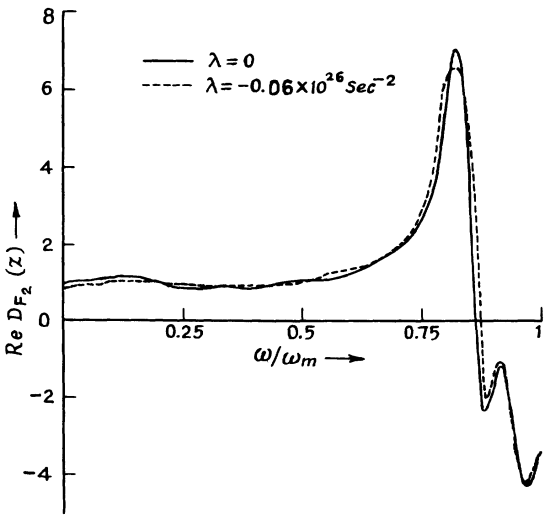

FIG. 6. Calculated real part of the resonance denominator in F_2 mode.

a result totally different from that of Sennett *et al.*[21] However, we find an antiresonance at about 145 cm^{-1} of width 72 cm^{-1} in the high-frequency region which will be inaccessible to the experimental observation. The calculated one-phonon density of states (Fig. 3) shows a peak at 62 cm^{-1} due to the critical point $K(\frac{3}{4}, \frac{3}{4}, 0)$ of the Brillouin zone. As the absorption spectrum reflects the appropriate projection of the density of states of the host lattice the weak peak at 61 cm^{-1} may be attributed to the impurity-activated one-phonon acoustic band. Similar impurity-activated one-phonon acoustic bands have been observed earlier in several other impurity-host systems.[17,20,46]

V. DISCUSSION AND CONCLUSIONS

We have obtained an explicit expression for the impurity-induced ir absorption for systems having zinc-blende-type crystal structure containing a low concentration of substitutional impurities. A numerical estimate has been made for a CdTe crystal doped with 0.03-mol% Be impurities and compared with the experimental absorption. The general features of the observed absorption spectrum have been explained very well on the basis of a simplified central-force model. This model is physically significant in the sense that it involves only one adjustable parameter. The absorption peak at 61 cm^{-1} arises as an activated peak in the density of states of the host CdTe rather than as a resonant mode of Be impurity. We have also made calculations for the absorption due to some other isoelectronic impurities (viz., S,[23] Mg,[24,25] Mg and Al) and have observed the impurity-activated peak at 62 cm^{-1} in all cases. In the CdTe:Be system the shape and the peak of the absorption curve is reproduced well; however, the calculated absorption exhibits a relatively broad peak. It may be ascribed to the broadness of the calculated density of states. For an impurity ion with a polarizability different from the host ion it replaces, one may expect changes in the effective charges of the defect and its neighbors. The value of Szigetti's effective charge e^*_{eff} may be different in the doped crystal. In the present calculation, we have assumed a value of effective charge $e^*_{eff} = 0.72$ for the doped crystal, a value which is found in the pure CdTe crystal.

We may thus conclude that in the absence of the neutron scattering results for the lattice phonons the observed impurity-induced infrared absorption spectrum of a zinc-blende-type crystal can well be accounted for if we employ a simplified central-force model.

ACKNOWLEDGMENTS

The authors wish to express their sincere thanks to Dr. Y. P. Varshni, Dr. A. Grimm, Dr. S. S. Mitra, and Dr. J. F. Vetelino for their interest in the present work. Thanks are owed to the Council of Scientific and Industrial Research, and University Grants Commission, New Delhi, India, for their financial assistance. One of us (D. N. T.) is thankful to Dr. P. N. Ram for stimulating discussions. All numerical calculations were carried out on IBM 7044/1401 computers installed at the Indian Institute of Technology, Kanpur.

---

*UGC research fellow.

[1]M. V. Klein, in *Physics of Color Centers*, edited by W. G. Fowler (Academic , New York, 1968), Chap. 7, p. 429.

[2]A. A. Maradudin, in *Solid State Physics*, edited by F. Seitz and D. Turnbull (Academic, New York 1966), Vol. 19, p. 1.

[3]D. W. Berreman, Phys, Rev. 130, 2193 (1963).

[4]A. J. Sievers, in *Proceedings of the International Conference on Localized Excitations in Solids*, edited by R. F. Wallis (Plenum, New York, 1968), p. 27.

[5]W. Hayes, in Ref. 4, p. 140.

[6]W. G. Spitzer, in *Optical Properties of III-V Compounds*, edited by R. K. Willardson and A. C. Beers (Academic, New York, 1967), p. 17.

[7]D. L. Stierwalt and R. F. Potter, in Ref. 6, p. 71.

[8]A. Mitsuishi, in paper presented at U. S.-Japan Cooperative Seminar on Far Infrared Spectroscopy, Columbus, Ohio, 1965 (unpublished).

[9]O. M. Stafsudd, F. A. Haak, and K. Radisavljevic, J. Opt. Soc. Am. 57, 1475 (1967).

[10]G. L. Bottger and A. L. Geddes, J. Chem. Phys. 47, 4858 (1967).

[11]A. S. Barker, Jr., Phys. Rev. 165, 917 (1968).

[12]C. J. Johnson, G. H. Sherman, and R. Weil, Appl. Opt. 8, 1667 (1969).

[13]S. J. Fray, F. A. Johnson, and R. H. Jones, Proc. Phys. Soc. Lond. 76, 939 (1960).

[14]A. Hadni, J. Claudel, X. Gerbaux, G. Morlot, and J. M. Munier, Appl. Opt. 4, 487 (1965).

[15]S. S. Mitra, J. Phys. Soc. Jap. Suppl. 21, 61 (1966).

[16]A. Hadni, J. Claudel, and P. Strimer, Phys. Status Solidi 26, 241 (1968).

[17]J. Vallin, G. A. Slack, S. Roberts, and A. E. Hughes, Solid State Commun. 7, 1211 (1969); Phys. Rev. B 2, 4313 (1970).

[18]A. Manbe, A. Mitsuishi, H. Yoshinaga, Y. Ueda, and H. Sei, Tech. Rep. Osaka Univ. (Japan) 17, 263 (1967).

[19]A. Mooradian and G. B. Wright, in *Ninth International Conference on the Physics of Semiconductors*, edited by S. M. Ryvkin (Nauka, Leningrad, 1968), p. 1020.

[20]G. A. Slack, S. Roberts, and J. T. Vallin, Phys. Rev. 187, 511 (1969).

[21]C. T. Sennett, D. R. Bosomworth, W. Hayes, and A. R. L. Spray, J. Phys. C 2, 1137 (1969).

[22]J. L. T. Waugh and G. Dolling, Phys. Rev. 132, 2410

(1963); G. Dolling and J. L. T. Waugh, in *Proceedings of the International Conference on Lattice Dynamics, Copenhagen, Denmark*, 1963, edited by R. F. Wallis (Pergamon, London, 1965), p. 19.
[23]J. L. Yarnell, J. L. Warren, R. G. Wenzel, and P. J. Dean, in Proceedings of the Conference on Inelastic Neutron Scattering, Copenhagen, Denmark, 1968 (unpublished).
[24]L. A. Feldkamp, G. Venktaraman, and J. S. King, Solid State Commun. 7, 1571 (1969); L. A. Feldkamp, thesis (University of Michigan, 1969) (unpublished).
[25]J. Bergsma, Phys. Lett. A 32, 324 (1970).
[26]B. Hennion, F. Moussa, G. Pepy, and K. Kunc, Phys. Lett. A 36, 376 (1971).
[27]D. L. Price, J. M. Rowe, and R. M. Nicklow, Phys. Rev. B 3, 1268 (1971).
[28]C. Carabatos, B. Hennion, K. Kunc, F. Moussa, and C. Schwab, Phys. Rev. Lett. 26, 770 (1971).
[29]B. Hennion, F. Moussa, B. Prevot, C. Carabatos, and C. Schwab, Phys. Rev. Lett. 28, 964 (1972).
[30]A. K. Rajagopal and R. Srinivasan, Z. Phys. 158, 471 (1960).
[31]J. F. Vetelino, S. S. Mitra, and K. V. Namjoshi, Phys. Rev. B 2, 967 (1970).
[32]J. F. Vetelino and S. S. Mitra, Solid State Commun. 7, 1181 (1969).
[33]J. F. Vetelino, S. S. Mitra, O. Brafman, and T. C. Damen, Solid State Commun. 7, 1809 (1969).
[34]R. Banerjee and Y. P. Varshni, Can. J. Phys. 47, 451 (1969); J. Phys. Soc. Jap. 30, 1015 (1971); Solid State Commun. 10, 2801 (1971).
[35]D. N. Talwar and Bal K. Agrawal, Solid State Commun. 11, 1691 (1972).
[36]D. N. Talwar and Bal K. Agrawal, Phys. Rev. B 8, 693 (1973).
[37]D. N. Talwar and Bal K. Agrawal, Phys. Status Solidi (to be published).
[38]B. G. Dick, in *Lattice Dynamics*, edited by R. F. Wallis (Pergamon, London, 1965), p. 159.
[39]W. Cochran, in Rev. 38, p. 75.
[40]H. M. J. Smith, Phil. Trans. R. Soc. (Lond.) A 241, 105 (1948).
[41]A. Grimm, A. A. Maradudin, I. P. Ipatova, and A. V. Subashiev, J. Phys. Chem. Solids 33, 775 (1972).
[42]D. N. Talwar and Bal K. Agrawal, Solid State Commun. 14, 25 (1974).
[43]D. N. Talwar and Bal K. Agrawal, Phys. Rev. B 15 (1974).
[44]A. Manabe, Y. Ikuta, A. Mitsuishi, H. Komiya, and S. Ibuki, Solid State Commun. 9, 1499 (1971).
[45]A. Mitsuishi and A. Manabe, Oyo Butsuri 41, 7 (1972).
[46]P. N. Ram, Ph.D. thesis (Univ. of Allahabad, Allahabad, 1972) (unpublished).
[47]P. N. Ram and Bal K. Agrawal, J. Phys. Chem. Solids 33, 957 (1972).
[48]B. Szigetti, Trans. Faraday Soc. 45, 155 (1949).
[49]W. Ludwig, in *Ergebnisse der exakten Naturwissenschaften*, edited by S. Flügge and F. Trendelenburg (Springer–Verlag, Berlin 1964) Vol. 35, p. 1.
[50]E. W. Kellerman, Philos. Trans. R. Soc. Lond. A 178, 17 (1941); 238, 513 (1940).
[51]R. H. Lyddane, R. G. Sachs, and E. Teller, Phys. Rev. 59, 673 (1941).
[52]R. Beserman and M. Balkanski (private communication).
[53]M. Krauzman, C. R. Acad. Sci. B 264, 1117 (1967).
[54]W. Tayler, Phys. Lett. A 24, 556 (1967).
[55]S. Ushioda, A. Pinczuk, W. Taylor, and E. Burstein, in *II-VI Semiconducting Compounds*, edited by D. G. Thomas (Benjamin, New York, 1967), p. 1185.
[56]W. G. Nilsen, in *Light Scattering Spectra of Solids*, edited by G. B. Wright (Springer–Verlag, New York, 1969), p. 129.
[57]H. J. McSkimin, J. Appl. Phys. 24, 988 (1953).
[58]R. Brout, Phys. Rev. 113, 43 (1959).
[59]A. J. Sievers, A. A. Maradudin, and S. S. Jaswal, Phys. Rev. 138, A272 (1965).
[60]Y. Ikuta, A. Manabe, A. Mitsuishi, H. Komiya, and S. Ibuki, Opt. Commun. 5, 285 (1972).